An analysis of recent BLYP and PBE-based range-separated double-hybrid density functional approximations for main-group thermochemistry, kinetics and noncovalent interactions

Asim Najibi, Marcos Casanova-Páez, and Lars Goerigk*

School of Chemistry, The University of Melbourne, Parkville, Australia;

Ph: +61-(0)3-83446784

E-mail: lars.goerigk@unimelb.edu.au

Abstract

We investigate the effects of range separation of the exchange energy on electronic ground-state properties for recently published double-hybrid density functionals (DHDFs) with the extensive GMTKN55 database for general main-group thermochemistry, kinetics and noncovalent interactions. We include the semi-empirical range-separated DHDFs ωB2PLYP and ωB2GP-PLYP developed by our group for excitation energies, together with their ground-state-parametrized variants, which we denote herein as ωB2PLYP18 and ωB2GP-PLYP18. We also include the non-empirical range-separated DHDFs RSX-0DH and RSX-QIDH. For all six DHDFs, damping parameters for the DFT-D3 dispersion correction (and for its DFT-D4 variant) are presented. We comment on when the range-separated functionals can be more beneficial than their global counterparts, and conclude that range separation alone is no guarantee for overall improved results. We observe that the BLYP-based functionals generally outperform

1

the PBE-based functionals. We finally note that the best-performing double-hybrid density functionals for GMTKN55 are still the semi-empirical range-separated double hybrids ωDSD3-PBEP86-D4 and ωDSD$_{72}$-PBEP86-D4, the former of which includes a third-order perturbative correlation term in addition to the more conventional second-order perturbation that DHDFs are based upon.

1   Introduction

Kohn-Sham Density Functional Theory[1] (DFT) is, without a doubt, the main quantum-chemical methodology utilized for computational molecular calculations due to its efficiency and accuracy. While in principle an exact theory, all applicable computational methods within the KS-DFT framework are known as density functional approximations (DFAs). Comprehensive benchmark studies have helped identifying the most robust and widely applicable DFAs,[2–7] while also revealing the lack of correlation between popularity and accuracy for some DFAs.[8] Double-hybrid density functionals (DHDFs),[9,10] which formally belong to the highest rung of the "Jacob's Ladder"[11] of DFT, make up the most-accurate class of DFAs for molecular chemistry, particularly for main-group systems.[2,4,5,12,13]

DHDFs are composed of semi-local exchange and correlation DFAs (E_X^{DFA} and E_C^{DFA}) combined with nonlocal Fock exchange (E_X^{HF}). Those three components provide molecular orbitals (MOs) and MO energies during the conventional self-consistent-field (SCF) step which are subsequently used to obtain a second-order perturbative (PT2) nonlocal correlation energy (E_C^{PT2}) resembling second-order Møller-Plesset perturbation theory, as defined by Grimme in 2006:[9]

$$E_{XC}^{DHDF} = a_x E_X^{HF} + a_{x,DFA} E_X^{DFA} + a_{c,DFA} E_C^{DFA} + a_c E_C^{PT2} \tag{1}$$

where $a_{x,DFA}$ and $a_{c,DFA}$ are scaling parameters for the DFT exchange and correlation energies, and a_x and a_c scaling parameters for Fock exchange and PT2 corre-

lation, respectively; usually, but not always, those parameter values depend on one another.[9,10,14–16]

Conventional hybrids and DHDFs that use the same electron-electron interaction operator over the entire range of interelectronic distance are often referred to as "global" hybrids and DHDFs. However, it has also been suggested to partition that operator into into short-range (SR) and long-range (LR) components:[17]

$$\frac{1}{|\mathbf{r} - \mathbf{r}'|} = \frac{1 - \mathrm{erf}(\omega\,|\mathbf{r} - \mathbf{r}'|)}{|\mathbf{r} - \mathbf{r}'|} + \frac{\mathrm{erf}(\omega\,|\mathbf{r} - \mathbf{r}'|)}{|\mathbf{r} - \mathbf{r}'|} \tag{2}$$

where the first and second terms account for the SR and LR interaction, respectively, $\mathbf{r}$ and $\mathbf{r}'$ are electronic spatial coordinates, erf is the error function, and ω controls the interplay between the SR and LR parts. When applying this idea to the the exchange components of hybrid or double-hybrid DFAs, the SR exchange is usually composed of both DFT and Fock exchange while the LR regime is governed entirely by Fock exchange, usually —but not always[18,19] — to 100% in the asymptotic region. This technique is applied to overcome the problem of the wrong decay of the exchange potential with increasing interelectronic distance. The exchange DFA can, thus, be written as:[17–31]

$$E_X(\omega) = a_x E_X^{HF,SR}(\omega) + a_{x,DFA} E_X^{DFA,SR}(\omega) + E_X^{HF,LR}(\omega) \tag{3}$$

Here, a_x and $a_{x,DFA}$ are the scaling parameters for the Fock and DFT short-range exchange energies, respectively (compare with Eq. 1). The resulting methods are known as range-separated (RS) DFAs; see Refs 31, 32, 33, 34, 35 and 36 for highly robust and accurate examples for ground-state thermochemistry. The range-separation idea has also occasionally been modified and applied in the context of wavefunction second-order perturbation theory or the PT2 term in DHDFs.[37–41] However, as the application of the range-separation idea is more common in exchange functionals, our present study only considers DHDFs that use the conventional PT2 term because this facilitates a direct comparison between the range-separated version of a DHDF and its

"parent", the global DHDF.

In this study, we focus on the applicability of six recently developed RS-DHDFs to ground-state thermochemistry, kinetics and noncovalent interactions. These six RS-DHDFs are ωB2PLYP,[42] ωB2GP-PLYP,[42] their variants ωB2PLYP18[42] and ωB2GP-PLYP18,[42] as well as RSX-0DH[43] and RSX-QIDH.[44] The semi-empirical methods ωB2PLYP and ωB2GP-PLYP are based on Becke-88[45] (B) exchange and Lee-Yang-Parr[46] (LYP) correlation and were parametrized by our group for electronic excitation energies.[42] They were shown to be some of the most accurate and robust time-dependent DFT methods for vertical singlet-singlet and singlet-triplet excitations, including local valence, Rydberg and charge-transfer transitions.[42,47–49] The value of the range-separation parameter ω is 0.30 bohr^{-1} for ωB2PLYP and 0.27 bohr^{-1} for ωB2GP-PLYP, which is similar to many RS hybrids.[18,28,30] During the development of both RS-DHDFs our group also attempted to fit the range-separation parameter to ground-state electron affinities (EAs) and ionization potentials (IPs) resulting in $\omega = 0.18$ bohr^{-1} in both cases.[42] Those methods did not seem promising for excitation energies and have since then never been applied again. For comparison reasons we test them in our study on ground-state properties and denote these versions as ωB2PLYP18 and ωB2GP-PLYP18. We compare the four ωB2(GP-)PLYP(18) methods with the two global DHDFs B2PLYP[9] and B2GP-PLYP,[50] upon which those RS-DHDFs are based. The "non-empirically" developed global DHDFs PBE0-DH[15] and PBE-QIDH[16]—which are based on Perdew-Burke-Ernzerhof[51] (PBE) exchange and correlation—have been turned into range-separated DFAs by fitting ω to the ground-state energy of the hydrogen atom, resulting in the RSX-0DH and RSX-QIDH methods, which have ω values of 0.33 and 0.27 bohr^{-1}, respectively.[43,44] The purpose of this choice of fit was to eliminate the self-interaction error (SIE) for the hydrogen atom, a strategy that has been shown beneficial for some other one-electron systems[52] as well as the SIE4x4[4] benchmark set for SIE-related problems.[43,44] Ground-state applications of the RSX-DHDFs have been limited to a handful of benchmark sets pertaining to thermochemistry, kinetics and noncovalent interactions, a handful of which the GMTKN55

database contains—albeit with sometimes different reference values—but yet without the addition of any London dispersion corrections.[43,53] The two RSX-DHDFs have also been applied to excitation energies, but were outperformed by other DFAs, including RS hybrids, global DHDFs and our RS-DHDFs ωB2PLYP and ωB2GP-PLYP.[47]

Due to the very good performance of our BLYP-based RS-DHDFs and the limited tests conducted on the RSX-DHDFs, our goal is to extensively assess them for ground-state problems. For that purpose we rely on the complete GMTKN55[4] database of general main-group thermochemistry, kinetics and noncovalent interactions. Note that B2PLYP, B2GP-PLYP, PBE0-DH and PBE-QIDH have been previously assessed on this database,[4,5] which allows us to analyze what the impact of range separation on those methods is. In addition, our numbers reported herein provide us with an opportunity to compare our RS-DHDFs and the RSX-DHDFs with thorough assessments of other RS-DHDFs on the same database, such as ωB97M(2)[34] and the spin-component scaled RS-DHDFs ωDSD3-PBEP86-D4[36] and ωDSD$_{72}$-PBEP86-D4,[35] with the first and second following different strategies compared to the original DHDF definition in Eq. 1. In the context of this study, we note that while several modern range-separated hybrid functionals may be accurate for ground-state properties, it cannot be definitely concluded that range separation alone guarantees improved performance when compared to results for global hybrids.[2–4,6,7] Herein we assess if this is also the case for RS-DHDFs. In order to allow a fair comparison with the more than 330 DFA variants assessed on GMTKN55 to date, we present new functional-specific damping parameters of various additive, Grimme-type London dispersion corrections with the main focus of our discussion being on the DFT-D3(BJ)[54,55] correction, as it is one of the currently most applied. The impact of this correction on the RS-DHDFs is briefly discussed. We also discuss the impact of the value of ω for the BLYP-based RS-DHDFs, and comment on the performance of the BLYP-based semi-empirical methods compared to the PBE-based "non-empirical" RSX-DHDFs.

2 Technical details

We conducted calculations for six DFAs, namely, ωB2PLYP, ωB2GP-PLYP, ωB2PLYP18, ωB2GP-PLYP18, RSX-0DH and RSX-QIDH. While those calculations were performed on a local version of ORCA4,[56,57] we would like to point out that the BLYP-based DFAs can additionally be used in ORCA version 4.2 and above, with the "18" variants requiring a manual definition of the ω value that overwrites the hardcoded values for ωB2(GP-)PLYP. The PBE-based RSX methods will be available in an upcoming release of ORCA. To allow comparison to the more than 330 methods tested by us on GMTKN55, we use the same settings as in those studies. This means the def2-QZVP[58] basis set was utilized, with ORCA's GRID3 and FINALGRID4 options and its SCFCONV7 convergence criterion. Dunning's diffuse s and p functions[59] were added to def2-QZVP for oxygen in the WATER27 benchmark set. Similarly, Dunning's diffuse s and p functions were utilized for all non-hydrogen atoms and diffuse s functions for H in the G21EA, AHB21 and IL16 benchmark sets. Core-electrons of the heavy elements in the HEAVY28, HEAVYSB11, and HAL59 benchmark sets were replaced with the def2-ECP[58] effective-core-potentials. The frozen-core approximation was used for all assessed double hybrids to prevent basis set superposition errors from core-core electron correlation.[60] The resolution of identity (RI)[61] approximation was used for the Coulomb integrals and for the PT2 correlation energy, utilizing the corresponding auxiliary basis sets in ORCA. We used the standalone DFT-D3 program[62] for the calculation of DFT-D3(BJ) dispersion energies for GMTKN55 and in the fitting procedure of the damping parameters for the DFAs. During this work, we experienced a handful of convergence issues. The systems for which this was the case were excluded from the statistical analyses for the given benchmark set with the given DFA. A list of the systems are shown in Section 4 of the SI.

The GMTKN55 database consists of 55 benchmark sets containing a total of 1505 relative energies; see Ref. 4 for a detailed list of all benchmark sets. Those 55 sets are part of 5 distinct subcategories, see Table 1. The analysis of the complete GMTKN55

Table 1: Subcategories of the GMTKN55 database and the number of their constituent benchmark sets.

subcategory	no. benchmark sets
basic properties and reactions of small systems	18
isomerizations and reactions of large systems	9
barrier heights	7
intermolecular noncovalent interactions[a]	12
intramolecular noncovalent interactions[a]	9

[a]The inter- and intramolecular noncovalent interactions can be combined to one overarching category.

and its subcategories is facilitated by the weighted total mean absolute deviation (WT-MAD) scheme presented in the original GMTKN55 study, which combines multiple mean absolute deviations (MADs) for the individual benchmark sets to one final number that allows the ranking of DFAs.[4] Two versions of the WTMAD idea were presented and herein we use the "WTMAD-2" scheme which has been defined as:

$$\text{WTMAD-2} = \frac{1}{\sum_i^{55} N_i} \sum_i^{55} \left(N_i \frac{56.84}{\overline{|\Delta E|}_i} \text{MAD}_i \right) , \tag{4}$$

where N_i is the number of data points in i^{th} benchmark set, $\overline{|\Delta E|}_i$ the average reference absolute energy of a benchmark set, and 56.84 kcal/mol the average of all 55 $\overline{|\Delta E|}_i$ values. Individual deviations of relative energies from reference values are defined as $E_{DFA}^{total} - E_{reference}^{total}$.

3 Results and discussion

3.1 Influence of a London dispersion correction

The s_6 parameter in DFT-D3, which scales the long-range component of the dispersion energy, was determined for all six RS-DHDFs according to the scheme presented by Goerigk and Grimme.[63] The Ne_2, Ar_2 and Kr_2 noncovalently bound dimers were considered at large interatomic distances to guarantee the interaction energies were governed entirely by long-range dispersion—7 Å for Ne_2, and 10 Å for Ar_2 and Kr_2.

The PT2 contributions—scaled by a_c—of the interaction energies of the three dimers were evaluated and compared to CCSD(T)[64]/aug-cc-pVTZ[59] dispersion energies. This allowed to gauge how much long-range dispersion was on average recovered by the DHDFs. That average was taken, and subtracted from unity to give s_6. This means that if a method reproduced the CCSD(T) long-range dispersion energies correctly, s_6 would be equal to zero; see Ref. 63 for more details on the reasoning behind the entire procedure. The resulting values are shown in Table 2 and they range from $s_6 = 0.595$ [ωB2GP-PLYP(18)] to 0.858 (RSX-0DH).

The remaining three DFT-D3(BJ) damping parameters were determined in a least-squares fit with the combined NCIBLIND,[65] S22x5[66] and S66x8[67] benchmark sets of noncovalent interaction energies. This has become the training set for the related DFT-D4[68,69] and various DFT-D3-type methods published since 2017.[4–6,68,69] The parameters and root mean square deviations (RMSDs) for the fit set are shown in Table 2 and extended statistical results of the fits are shown in Tables S3-6 in the SI. Details on the actual correction and the role of each parameter have been documented multiple time elsewhere and we refer, e.g., to Refs 55, 70, or 71 for details. We initially observed the s_8 values to be largely negative, without much change in RMSDs. The large negative values of s_8 would indicate an overestimation of medium-range dispersion. We constrained the s_8 values to zero in such cases, which has also been the case for other global and RSDHDFs.[35,36,72] Table 2 shows the RMSDs for the optimized parameters, together with the RMSDs of the dispersion-uncorrected DFAs. The RMSDs of RSX-0DH-D3(BJ) and RSX-QIDH-D3(BJ) are only slightly smaller than those of RSX-0DH and RSX-QIDH, respectively. In the case of ωB2(GP-)PLYP(18), the RMSDs do not change at all with the DFT-D3(BJ) correction. The effect of the DFT-D3(BJ) correction on the functionals is seen to a greater extent with the GMTKN55 database, which we discuss below.

The damping parameters and statistical analysis of the DFT-D3(0)[54] and DFT-D4 dispersion corrections are additionally shown in Tables S1-6. We see that the DFT-D3(0) and DFT-D4 corrections have basically the same effect on the DFAs as the

Table 2: DFT-D3(BJ) damping parameters for the six studied RS-DHDFs, root mean square deviations (RMSD) of the resulting dispersion-corrected functionals for the fit set as well as RMSDs for their uncorrected counterparts (kcal/mol).

functional	s_6	a_1	s_8	a_2	RMSD
RSX-0DH					1.06
RSX-0DH-D3(BJ)	0.858	-0.235	3.126	11.798	0.98
RSX-QIDH					0.77
RSX-QIDH-D3(BJ)	0.633	0.750	0.000	8.178	0.76
ωB2PLYP18					1.00
ωB2PLYP18-D3(BJ)	0.691	3.368	0.000	8.130	1.00
ωB2GP-PLYP18					0.87
ωB2GP-PLYP18-D3(BJ)	0.595	3.172	0.000	9.512	0.87
ωB2PLYP					0.85
ωB2PLYP-D3(BJ)	0.691	1.499	0.000	6.257	0.85
ωB2GP-PLYP					0.77
ωB2GP-PLYP-D3(BJ)	0.595	2.649	0.000	8.991	0.77

DFT-D3(BJ) correction, which is why we only discuss the latter in the remainder of this work, mostly due to the fact that most other of our previously published results for GMTKN55 are based on the DFT-D3(BJ) correction, too.

We present the WTMAD-2 values of all assessed functionals for the GMTKN55 database in Figure 1, Table 3, and Table S7. The WTMADs of PBE0-DH[-D3(BJ)] and PBE-QIDH[-D3(BJ)] were taken from Ref. 5 and those of B2PLYP[-D3(BJ)] and B2GP-PLYP[-D3(BJ)] from Ref. 4. We first note that the effect of the DFT-D3(BJ) dispersion correction is small for the RS-DHDFs assessed in this study. By contrast, the global DHDFs generally benefit greatly from a dispersion correction. The WTMAD-2 values over the entire GMTKN55 database are 8.13, and 5.54 kcal/mol for PBE0-DH and PBE0-DH-D3(BJ), whereas those of RSX-0DH and RSX-0DH-D3(BJ) are 9.22 and 9.24 kcal/mol, respectively. Similarly, PBE-QIDH and PBE-QIDH-D3(BJ) have WTMAD-2 values of 5.61 and 4.47 kcal/mol, whereas RSX-QIDH-D3(BJ) only improves by 0.11 kcal/mol over its uncorrected counterpart (6.88 vs. 6.99 kcal/mol). The values of B2PLYP and B2PLYP-D3(BJ) are 8.70 and 3.93 kcal/mol, while those of ωB2PLYP18 and ωB2PLYP18-D3(BJ) are both 6.54 kcal/mol, and those of ωB2PLYP and ωB2PLYP-D3(BJ) are 5.76 and 5.72 kcal/mol, respectively. The same trends

can also be observed for the B2GP-PLYP-based functionals (Table 3). It has also been noted that a dispersion correction has at times only a small impact on the performance of a RS-DHDF for the entire GMTKN55 database for ωB97X-2[31] when paired with the DFT-D3(BJ) and DFT-D3(0) corrections.[5]

The detailed breakdown of the impact of the DFT-D3(BJ) correction on the WTMAD-2s for the individual categories in GMTKN55 is shown in Figure 1. Here, we only comment on a handful of examples. For instance, it is worth noting that the DFT-D3(BJ) correction unanimously increases the WTMADs of the PBE-based methods for the basic properties and reactions of small systems subset (both for the global and range-separated variants) shown in Figure 1a. Looking specifically at the intermolecular and intramolecular noncovalent interaction categories, we see minor improvements in the WTMADs for RS-DHDFs with DFT-D3(BJ) with one exception, namely RSX-0DH for intermolecular noncovalent interactions. Here, the WTMAD-2 of RSX-0DH is 12.64 kcal/mol, whereas the WTMAD-2 of RSX-0DH-D3(BJ) is 14.15 kcal/mol. Comparing the mean deviations (MDs) of RSX-0DH and RSX-0DH-D3(BJ) for the constituent benchmark sets of the intermolecular noncovalent interactions subset, we do not observe a clear trend that would suggest a general under- or overestimation of the dispersion energy with the DFT-D3(BJ) correction (see Tables S8 and S9).

In summary, we can conclude that the impact of a dispersion correction on the herein tested RS-DHDFs seems to be marginal when applied to equilibrium geometries. However, with the exception of RSX-0DH, its application is not detrimental, and as such we recommend its usage by default.

3.2 The range-separation parameter in ωB2(GP-)PLYP

We compare the original ωB2PLYP and ωB2GP-PLYP DFAs, which have ω values of 0.30 and 0.27 bohr^{-1}, respectively, to ωB2PLYP18 and ωB2GP-PLYP18, which both have ω values of 0.18 bohr^{-1}. As also mentioned in the Introduction, ω was fitted using a set[73] of electronic excitation energies for ωB2PLYP and ωB2GP-PLYP.
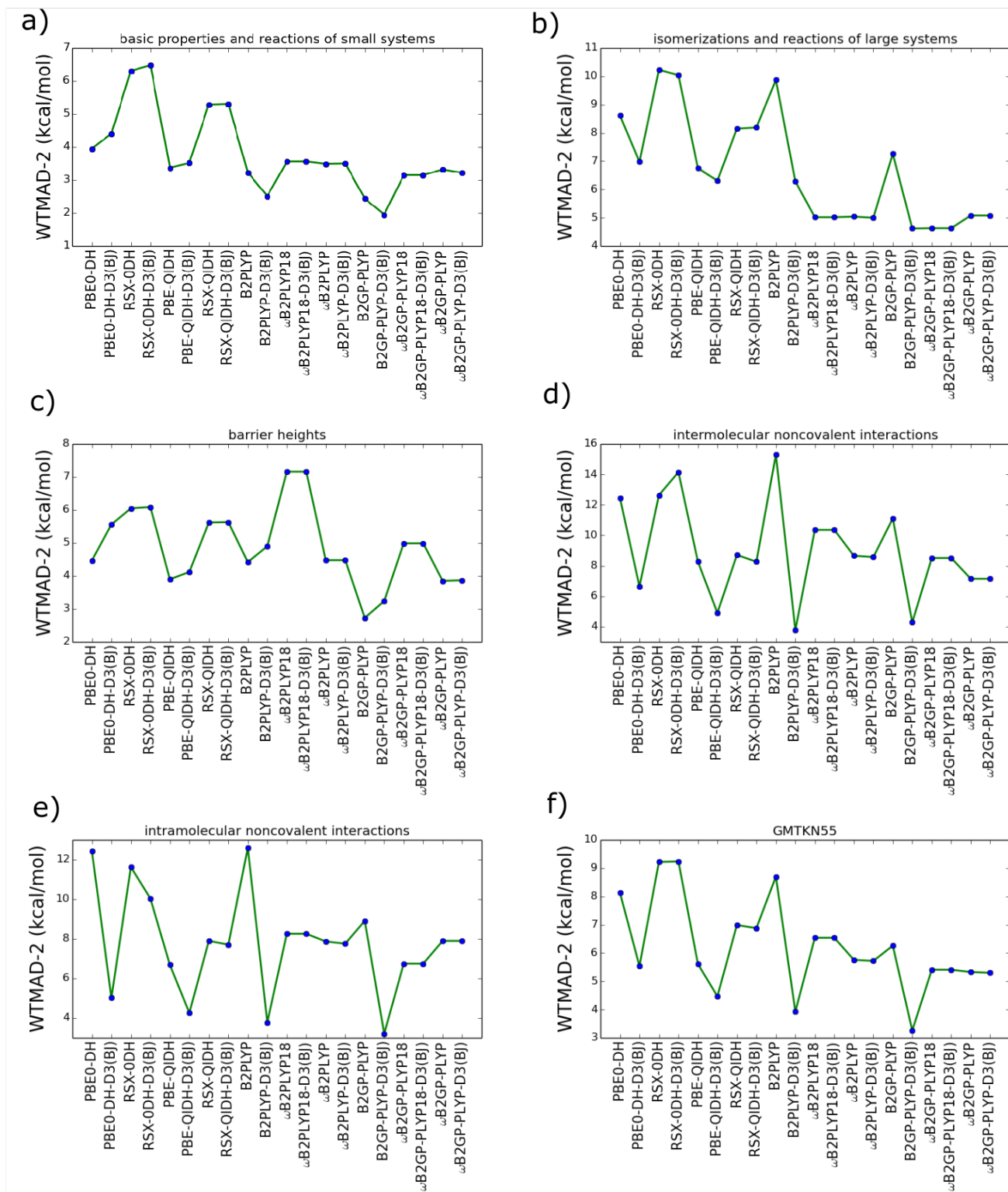
Figure 1: WTMAD-2 values (kcal/mol) for all assessed methods in this study. The values for GMTKN55 and its subsets are shown — a) basic properties and reaction energies of small systems, b) isomerization energies and reaction energies of large systems, c) barrier heights, d) intermolecular noncovalent interaction energies, e) intramolecular noncovalent interaction energies and f) GMTKN55. The line joining the data points is shown to guide the eye. PBE0-DH[-D3(BJ)] and PBE-QIDH[-D3(BJ)] values were taken from Ref. 5. B2PLYP[-D3(BJ)] and B2GP-PLYP[-D3(BJ)] values were taken from Ref. 4.

11

Table 3: Weighted mean absolute deviations (WTMAD-2) of all functionals assessed in this study for the complete GMTKN55 database (kcal/mol).

functional	WTMAD-2
PBE0-DH[a]	8.13
PBE0-DH-D3(BJ)[a]	5.54
RSX-0DH	9.22
RSX-0DH-D3(BJ)	9.24
PBE-QIDH[a]	5.61
PBE-QIDH-D3(BJ)[a]	4.47
RSX-QIDH	6.99
RSX-QIDH-D3(BJ)	6.88
B2PLYP[b]	8.70
B2PLYP-D3(BJ)[b]	3.93
ωB2PLYP18	6.54
ωB2PLYP18-D3(BJ)	6.54
ωB2PLYP	5.76
ωB2PLYP-D3(BJ)	5.72
B2GP-PLYP[b]	6.26
B2GP-PLYP-D3(BJ)[b]	3.26
ωB2GP-PLYP18	5.41
ωB2GP-PLYP18-D3(BJ)	5.41
ωB2GP-PLYP	5.33
ωB2GP-PLYP-D3(BJ)	5.30

[a]Taken from Ref. 5. [b]Taken from Ref. 4.

In the same study, it was separately fitted using ground-state ionization potentials (G21IP benchmark set in GMTKN55)[74,75] and electron affinities (G21EA benchmark set in GMTKN55),[74,75] giving ωB2PLYP18 and ωB2GP-PLYP18. The inspiration for the latter fit had been based on earlier studies of RS hybrids that tuned the range-separation parameters to EAs and IPs, such as Ref. 76. While the ωB2(GP-)PLYP18 approaches were abandoned very quickly during the study of excitation energies, we test them here again on the ground-state problems covered by GMTKN555.

First, we compare ωB2PLYP and ωB2GP-PLYP with ωB2PLYP18 and ωB2GP-PLYP18 for G21EA and G21IP. The MADs for G21EA are 2.43, 2.05, 1.38 and 1.96 kcal/mol, and those for G21IP are 2.17, 2.02, 2.17 and 1.98 kcal/mol, respectively. Hence, the two ω variants perform similarly for G21EA and G21IP, with the excep-

tion of ωB2PLYP18 outperforming ωB2PLYP for G21EA. This would be an indication of a relatively flat parameter potential for these two properties and DFAs. ωB2(GP-)PLYP perform noticeably better than ωB2(GP-)PLYP18 for the barrier heights subcategory of GMTKN55, with WTMAD-2(ωB2PLYP) = 4.48 kcal/mol and WTMAD-2(ωB2PLYP18) = 7.16 kcal/mol, and WTMAD-2(ωB2GP-PLYP) = 3.85 kcal/mol and WTMAD-2(ωB2GP-PLYP18) = 4.99 kcal/mol. The same is true for the intermolecular noncovalent interactions subset — WTMAD-2(ωB2PLYP) = 8.66 kcal/mol and WTMAD-2(ωB2PLYP18) = 10.36 kcal/mol, WTMAD-2(ωB2GP-PLYP) = 7.15 kcal/mol and WTMAD-2(ωB2GP-PLYP18) = 8.51 kcal/mol. ωB2PLYP also outperforms ωB2PLYP18 for the intramolecular noncovalent interactions with WTMAD-2 values of 7.87 and 8.26 kcal/mol respectively, whereas ωB2GP-PLYP underperforms compared to ωB2GP-PLYP18 with WTMAD-2 values of 7.90 and 6.75 kcal/mol. Overall, ωB2PLYP outperforms ωB2PLYP18 with WTMAD-2 values of 5.76 and 6.54 kcal/mol, respectively, for GMTKN55, while ωB2GP-PLYP and ωB2GP-PLYP18 perform similarly to each other with WTMAD-2 values of 5.33 and 5.41 kcal/mol, respectively. Here we reported WTMAD-2 values for the dispersion-uncorrected functionals, but the same trends can be observed for the dispersion-corrected variants (see Table S7).

3.3 Comparison of range-separated and global double hybrid functionals

In this section, we compare the six RS-DHDFs to their global counterparts. Overall, the global DHDFs outperform the range-separated ones. This can be seen from the WTMAD-2 values provided in Figure 1, Table 3, and Table S7. The WTMAD-2 values for the entire database for PBE0-DH-D3(BJ) and RSX-0DH-D3(BJ) are 5.54 and 9.24 kcal/mol and the GMTKN55 WTMAD-2 values for PBE-QIDH-D3(BJ) and RSX-QIDH-D3(BJ) are 4.47 and 6.88 kcal/mol. Similarly, the GMTKN55 WTMAD-2 values of B2PLYP-D3(BJ), ωB2PLYP18-D3(BJ) and ωB2PLYP-D3(BJ) are 3.93, 6.54

and 5.72 kcal/mol, and those of B2GP-PLYP-D3(BJ), ωB2GP-PLYP18-D3(BJ) and ωB2GP-PLYP-D3(BJ) 3.26, 5.41 and 5.30 kcal/mol, respectively.

Having stated the general trends, we discuss some benchmark-specific examples, as it might still be possible for range separation to have a positive influence for specific problems. For instance, we make some important observations for the SIE4x4 benchmark set of SIE-related problems, which consists of the dissociation curves of H_2^+, He_2^+, $(H_2O)_2^+$ and $(NH_3)_2^+$, as well as for and the DC13 set of "difficult cases", such as the formation of S_8 from S_2 and the 1,3-dipolar cycloaddition between ethene and diazomethane. Both benchmark sets belong to the GMTKN55 category that deals with basic properties and reaction energies of small systems. We chose those two benchmark sets for our discussion, as we see opposite trends when comparing the global and range-separated functionals. Looking at SIE4x4, we observe an improvement of the range-separated functionals in comparison to their global counterparts. The MADs of PBE0-DH-D3(BJ) and PBE-QIDH-D3(BJ) are 7.57 kcal/mol and 3.45 kcal/mol, respectively, whereas those of RSX-0DH-D3(BJ) and RSX-QIDH-D3(BJ) are 3.47 kcal/mol and 1.97 kcal/mol. This finding aligns well with previous studies of these functionals.[43,44] Similarly, the MAD of B2PLYP-D3(BJ) is 10.08 kcal/mol, whereas the MADs of ωB2PLYP18-D3(BJ) and ωB2PLYP-D3(BJ) are 8.74 kcal/mol and 5.98 kcal/mol, respectively. Lastly, the MAD of B2GP-PLYP-D3(BJ) is 6.56 kcal/mol, whereas ωB2GP-PLYP18-D3(BJ) and ωB2GP-PLYP-D3(BJ) have MADs of 5.72 kcal/mol and 4.16 kcal/mol. These results are consistent with the notion that range separation reduces the SIE, one of the main motivations of the development of range-separated functionals.[25,28,43,44,52] Looking at the DC13 benchmark set of difficult cases for DFT, we observe differing behaviors of the BLYP- and PBE-based range-separated functionals relative to their global counterparts. ωB2PLYP18-D3(BJ) and ωB2PLYP-D3(BJ) improve over B2PLYP-D3(BJ) — the MAD of B2PLYP-D3(BJ) is 6.77 kcal/mol, and those of ωB2PLYP18-D3(BJ) and ωB2PLYP-D3(BJ) are 3.69 kcal/mol and 5.08 kcal/mol, respectively. ωB2GP-PLYP18-D3(BJ) and ωB2GP-PLYP-D3(BJ) perform similarly to B2GP-PLYP-D3(BJ), with MADs of 4.13, 4.41 and 5.60 kcal/mol, respectively. By

contrast, the PBE-based range-separated methods deteriorate compared to their global counterparts. PBE0-DH-D3(BJ) and PBE-QIDH-D3(BJ) have MADs of 9.58 kcal/mol and 8.44 kcal/mol, whereas those of RSX-0DH-D3(BJ) and RSX-QIDH-D3(BJ) are 17.41 kcal/mol and 14.61 kcal/mol.

We see some improvements of the BLYP-based RS-DHDFs over the global counterparts for some benchmark sets of the "isomerizations and reactions of large systems" category. For instance, the MADs of B2PLYP-D3(BJ) and ωB2PLYP18-D3(BJ) for the set of C_{60} isomers (C60ISO), are 6.76 and 3.18 kcal/mol. This is a significant finding, as such systems have been reported to be difficult to treat with DHDFs.[4] The MADs for the bond-separation reactions of saturated hydrocarbons (BSR36) for B2GP-PLYP-D3(BJ) and ωB2GP-PLYP-D3(BJ) are 2.08 and 0.62 kcal/mol, with the latter sharing the same MAD as PBE0-2-D3(BJ),[10,77] to our knowledge the best DHDF for this benchmark set;[5] note that some articles on DHDFs tested on GMTKN55 do not always report all individual MADs.[12,13,35,36] Lastly, we note that ωB2PLYP18-D3(BJ) and ωB2PLYP-D3(BJ) outperform B2PLYP-D3(BJ) for this entire subcategory, with WTMAD-2 values of 5.02, 5.00 and 6.28 kcal/mol, respectively. By contrast, RSX-0DH-D3(BJ) and RSX-QIDH-D3(BJ) perform more poorly than PBE0-DH-D3(BJ) and PBE-QIDH-D3(BJ) for the isomerizations and reactions of large systems; their WTMAD-2 values are 10.04, 8.19, 6.98 and 6.31 kcal/mol. The only exception is the BSR36 set for which RSX-QIDH and RSX-QIDH-D3(BJ) are the best-performing functionals assessed in this study, with MADs of 0.44 and 0.50 kcal/mol, respectively (see Tables S11 and S12). They surpass the previously mentioned best DHDFs assessed for this benchmark set, namely PBE0-2-D3(BJ) and ωB2GP-PLYP-D3(BJ).

The assessed range-separated functionals deteriorate for the interaction energies of water clusters (WATER27). Here, the MADs of PBE0-DH-D3(BJ), PBE-QIDH-D3(BJ), B2PLYP-D3(BJ) and B2GP-PLYP-D3(BJ) are 4.11, 2.07, 2.03 and 1.87 kcal/mol, and by comparison, the MADs of RSX-0DH-D3(BJ), RSX-QIDH-D3(BJ), ωB2PLYP18-D3(BJ), ωB2PLYP-D3(BJ), ωB2GP-PLYP18-D3(BJ) and ωB2GP-PLYP-D3(BJ) are 8.32, 6.96, 15.60, 13.00, 12.49 and 11.27 kcal/mol.

This deterioration can be attributed to the large overestimation of the interaction energies of the water clusters, based on their large positive MDs. The MDs of PBE0-DH-D3(BJ), PBE-QIDH-D3(BJ), B2PLYP-D3(BJ) and B2GP-PLYP-D3(BJ) are 3.75, 1.76, 1.78 and 1.67 kcal/mol, whereas those of RSX-0DH-D3(BJ), RSX-QIDH-D3(BJ), ωB2PLYP18-D3(BJ), ωB2PLYP-D3(BJ), ωB2GP-PLYP18-D3(BJ) and ωB2GP-PLYP-D3(BJ) are 7.79, 6.56, 15.18, 12.65, 12.18 and 11.00 kcal/mol. The deterioration of the range-separated functionals for WATER27 is slightly surprising — Burke and coworkers suggested that Hartree-Fock densities could resolve density errors of DFAs, and so range-separated hybrid functionals should be affected to a smaller extent due to their 100% Fock exchange in the long-range regime.[78] In fact, they showed that the range-separated hybrid functional ωB97M-V has the smallest density errors for WATER27 compared to several GGA, meta-GGA, global hybrid and double hybrid DFAs. For one-electron systems, ωB2(GP-)PLYP and RSX-QIDH also had very small density errors.[52] Contrary to that, the 100% long-range Fock exchange of the RS-DHDFs presented in this study does not seem to successfully counteract DFA errors for the interaction energies of the water clusters in the WATER27 benchmark set. We would also like to draw attention to a recent study on density-corrected DFT for GMTKN55 that came to the conclusion that range-separated functionals and global DHDFs should not suffer greatly from the density error for WATER27 and other test sets due to their large proportion of Fock exchange.[79] Our results for this test set therefore seem to be influenced by other factors than the density error.

Looking at the barrier heights category, we expect the range-separated functionals to be more beneficial to treat the SIE-prone transition states containing elongated bonds. We see relatively good performance of ωB2PLYP[-D3(BJ)] and ωB2GP-PLYP[-D3(BJ)], compared to the other range-separated double hybrids. The WTMAD-2 values of ωB2PLYP-D3(BJ) and ωB2GP-PLYP-D3(BJ) are 4.48 and 3.87 kcal/mol, respectively. In fact, they both surpass B2PLYP-D3(BJ) in accuracy, which has a WTMAD-2 value of 4.90 kcal/mol. However, the other range-separated double hybrids have higher WTMAD-2 values compared to their global variants (see Figure 1c and

Table S7).

The effect of range separation may be irrelevant to many chemical problems in GMTKN55, rendering the global DHDFs to be more robust than the range-separated DHDFs. Nevertheless, attention is warranted towards the use of the range-separated DHDFs for self-interaction-error-related problems such as in SIE4x4, barrier heights, and even for other chemical problems represented by the "basic properties and reactions of small systems" and "isomerizations and reactions of large systems" subsets.

3.4 Comparison of "non-empirical" and semi-empirical double hybrid functionals

We remind the reader that RSX-0DH and RSX-QIDH have been advertised as "non-empirically" parametrized functionals, whereas ωB2PLYP(18) and ωB2GP-PLYP(18) are semi-empirically parametrized functionals. Our group previously presented a thorough analysis of the performance of non-empirical and semi-empirical DHDFs, showing that the best-performing double-hybrid functionals were semi-empirically parametrized.[5] We find that this is also the case for RSX-0/QIDH and ωB2(-GP)PLYP(18). The GMTKN55 WTMAD-2 values for RSX-0DH-D3(BJ) and RSX-QIDH-D3(BJ) are 9.24 and 6.88 kcal/mol respectively, whereas those for ωB2PLYP18-D3(BJ), ωB2PLYP-D3(BJ), ωB2GP-PLYP18-D3(BJ) and ωB2GP-PLYP-D3(BJ) are 6.54, 5.72, 5.41 and 5.30 kcal/mol (see Figure 1f and Table 3). Figure 1a-e and Table S7 also show that this trend occurs for the subcategories of GMTKN55. We also note that the BLYP-based functionals outperform the PBE-based ones, both in the case of the tested range-separated and global double-hybrid functionals; for instance, the GMTKN55 WTMAD-2 values of PBE0-DH-D3(BJ) and PBE-QIDH-D3(BJ) were reported to be 5.54 and 4.47 kcal/mol,[5] whereas those of B2PLYP-D3(BJ) and B2GP-PLYP-D3(BJ) were reported to be 3.93 and 3.26 kcal/mol.[4] In our previous studies on excitation energies, one could have argued that the superior performance of the BLYP-based RS-DHDF is due to them having been fitted to that same property.[47]

However, we see the same trend for ground-state properties, which should have been the domain of the RSX-DHDFs.

3.5 Comparison to previous GMTKN55 benchmark studies

Our study focuses on the use of range-separated double-hybrid functionals, and we saw some situations for which the partitioning of the exchange energy into the SR mixture of DFT and Fock exchange and LR Fock exchange is beneficial. However, we note that the RS-DHDFs examined in this study are still outperformed by the most recently assessed best-performing functionals for GMTKN55.[12,35,36] This assessment is based on the MADs for each benchmark set. This means that even after having added six more DFAs to the large body of GMTKN55-based data, the top-three double hybrid functionals based on WTMADs remain unchanged for GMTKN55 and its subcategories. Our findings may suggest that range-separated double-hybrid functionals may not stand out as a group over global double hybrids, despite, for example, ωB97X-2-D3(BJ),[31] ωB97M(2),[34] ωDSD$_{72}$-PBEP86-D4[35] and ωDSD3-PBEP86-D4[36] (which includes third-order perturbation) being ranked as leading DFAs in successive studies.[5,12,35,36] They have GMTKN55 WTMAD-2 values of 2.97, 2.19, 2.08 and 1.76 kcal/mol, respectively. Note that slightly different basis sets have been used in those studies, but the overall trends should still be comparable to numbers published with the benchmark sets used in our previous and the present GMTKN55 studies. Many range-separated hybrid and double-hybrid functionals have been developed with a refitting of the exchange and correlation scaling factors in addition to the optimization of the range-separation parameter ω.[32–36] This approach has proven to be successful, giving rise to the best hybrids and double hybrids, such as the ωB97X-V[32] and ωB97M-V[33] hybrid functionals and the DHDFs mentioned above. In our study, we wished to investigate the effect of range separation alone, which is why we kept the exchange and correlation scaling factors of the ωB2(GP-)PLYP(18) family of function-

als fixed with respect to their parent global DFAs, which was also the approach for the development of RSX-0DH and RSX-QIDH. The performance of all of the range-separated double hybrids assessed in our study falls within the performance range of double hybrids in general.[5,12,35,36] Amongst the range-separated double hybrid functionals assessed in our study, ωB2GP-PLYP-D3(BJ) and ωB2GP-PLYP18-D3(BJ) are overall best-performing, with GMTKN55 WTMAD-2 values of 5.30 and 5.41 kcal/mol. In summary, while a specifically well performing DFA may be range-separated, ranges eparation itself if no guarantee that a DFA really improves. This mirrors previous findings on ground-state properties.[2,4] Instead, the good results for a specific DFA are the consequence of the interplay between all of its individual components. As with all developments based on a trial-and-error approach, detailed benchmark studies have to be conducted before final recommendations can be made.

4   Summary and Conclusions

We investigated six recently published range-separated double-hybrid density functional approximations for electronic ground-state properties. Four of them were based on the BLYP exchange-correlation expressions and originally developed for the treatment of electronic excitation energies, namely ωB2PLYP, ωB2GP-PLYP, ωB2PLYP18, and ωB2GP-PLYP18. Two were PBE-based and "non-empirical" approximations fitted against the hydrogen-atom energy, namely RSX-0DH and RSX-QIDH. This was the first study of ground-state problems for the BLYP-based ones and the most comprehensive ground-state study of the PBE-based ones. For all six methods, we presented dispersion-correction parameters of the DFT-D3 and DFT-D4 types to allow for a fair comparison with other density functional approximations. Our assessment was based on the large GMTKN55 database for general main-group thermochemistry, kinetics and noncovalent interactions, which consists of 55 benchmark sets and a total of 1505 relative energies. We also included previously published[4,5] data of the global double-hybrid counterparts B2PLYP, B2GP-PLYP, PBE0-DH and PBE-QIDH, and

their dispersion-corrected versions.

We found that while the global double hybrids generally outperform their range-separated counterparts, many important observations were made in which the range-separated functionals proved to be beneficial. The prime example is the self-interaction error benchmark set SIE4x4, for which all the range-separated functionals outperform their global counterparts. Similarly, ωB2(GP-)PLYP(18) outperforms B2(GP-)PLYP for DC13, the benchmark set of known difficult cases for DFAs. Lastly, we note that the WTMADs of ωB2PLYP-D3(BJ) and ωB2PLYP18-D3(BJ) are noticeably lower than B2PLYP-D3(BJ) for the 'isomerizations and reactions of large systems' subset of GMTKN55. We see that the semi-empirical BLYP-based functionals generally outperform the non-empirical PBE-based functionals across GMTKN55, for both the range-separated and global functionals. This mirrors recent findings on electronic excitation energies for ωB2(GP-)PLYP and RSX-0/QIDH.[47] We see that the effect of the DFT-D3(BJ) correction on the assessed range-separated functionals is small, in contrast to their global counterparts, something that has also been observed for other range-separated double hybrids.[5] That being said, all assessed systems were in their equilibrium geometries. Given that the long-range scale parameter s_6 in the DFT-D3 correction was still relatively sizable, future investigations could focus on discussing non-equilibrium structures.

Overall, we see that range separation alone is no guarantee for the success of a functional but also depends on the underlying exchange-correlation expressions, something that was also seen in previously published studies on range-separated hybrids.[2,4] We note that the best-performing double-hybrid density functionals based on GMTKN55 is still the spin-component-scaled, semi-empirical range-separated DHDFs ωDSD3-PBEP86-D4 and ωDSD$_{72}$-PBEP86-D4, the former of which includes a third-order perturbative correlation term in addition to the more conventional second-order perturbation that DHDFs are based upon.

Acknowledgement

Notes

The authors declare no competing financial interest.

Supporting Information Available

The SI contains damping parameters for the DFT-D3(0) and DFT-D4 corrections; all relevant statistical data for the dispersion correction training set; all statistical data for GMTKN55; list of calculations with convergence problems.

References

(1) Kohn, W.; Sham, L. J. Self-consistent equations including exchange and correlation effects. *Phys. Rev.* **1965**, *140*, A1133–A1138.

(2) Goerigk, L.; Grimme, S. A thorough benchmark of density functional methods for general main group thermochemistry, kinetics, and noncovalent interactions. *Phys. Chem. Chem. Phys.* **2011**, *13*, 6670–6688.

(3) Mardirossian, N.; Head-Gordon, M. Thirty years of density functional theory in computational chemistry: an overview and extensive assessment of 200 density functionals. *Mol. Phys.* **2017**, *115*, 2315–2372.

(4) Goerigk, L.; Hansen, A.; Bauer, C.; Ehrlich, S.; Najibi, A.; Grimme, S. A look at the density functional theory zoo with the advanced GMTKN55 database for general main group thermochemistry, kinetics and noncovalent interactions. *Phys. Chem. Chem. Phys.* **2017**, *19*, 32184–32215.

(5) Mehta, N.; Casanova-Páez, M.; Goerigk, L. Semi-empirical or non-empirical double-hybrid density functionals: which are more robust? *Phys. Chem. Chem. Phys.* **2018**, *20*, 23175–23194.

(6) Najibi, A.; Goerigk, L. The nonlocal kernel in van der Waals density functionals as an additive correction: An extensive analysis with special emphasis on the B97M-V and ωB97M-V approaches. *J. Chem. Theory Comput.* **2018**, *14*, 5725–5738.

(7) Najibi, A.; Goerigk, L. DFT-D4 counterparts of leading meta-generalized-gradient approximation and hybrid density functionals for energetics and geometries. *J. Comput. Chem.* **2020**, *41*, 2562–2572.

(8) Goerigk, L.; Mehta, N. A trip to the density functional theory zoo: warnings and recommendations for the user. *Aust. J. Chem.* **2019**, *72*, 563–573.

(9) Grimme, S. Semiempirical hybrid functional with perturbative second-order correlation. *J. Chem. Phys.* **2006**, *124*, 034108.

(10) Goerigk, L.; Grimme, S. Double-hybrid density functionals. *Wiley Interdiscip. Rev. Comput. Mol. Sci.* **2014**, *4*, 576–600.

(11) Perdew, J. P.; Schmidt, K. Jacob's ladder of density functional approximations for the exchange-correlation energy. *AIP Conference Proceedings* **2001**, *577*, 1–20.

(12) Santra, G.; Sylvetsky, N.; Martin, J. M. L. Minimally Empirical Double-hybrid functionals trained against the GMTKN55 database: revDSD-PBEP86-D4, revDOD-PBE-D4, and DOD-SCAN-D4. *J. Phys. Chem. A* **2019**, *123*, 5129–5143.

(13) Martin, J. M. L.; Santra, G. Empirical double-hybrid density functional theory: A 'third way' in between WFT and DFT. *Isr. J. Chem.* **2020**, *60*, 787–804.

(14) Sharkas, K.; Toulouse, J.; Savin, A. Double-hybrid density-functional theory made rigorous. *J. Chem. Phys.* **2011**, *134*, 064113.

(15) Brémond, E.; Adamo, C. Seeking for parameter-free double-hybrid functionals: The PBE0-DH model. *J. Chem. Phys.* **2011**, *135*, 024106.

(16) Brémond, E.; Sancho-García, J. C.; Pérez-Jiménez, A. J.; Adamo, C. Communication: Double-hybrid functionals from adiabatic-connection: The QIDH model. *J. Chem. Phys.* **2014**, *141*, 031101.

(17) Leininger, T.; Stoll, H.; Werner, H.-J.; Savin, A. Combining long-range configuration interaction with short-range density functionals. *Chem. Phys. Lett.* **1997**, *275*, 151 – 160.

(18) Yanai, T.; Tew, D. P.; Handy, N. C. A new hybrid exchange-correlation functional using the Coulomb-attenuating method (CAM-B3LYP). *Chem. Phys. Lett.* **2004**, *393*, 51–57.

(19) Heyd, J.; Scuseria, G. E.; Ernzerhof, M. Erratum: Hybrid functionals based on a screened Coulomb potential [J. Chem. Phys. 118, 8207 (2003)]. *J. Chem. Phys* **2006**, *124*, 219906.

(20) Baer, R.; Neuhauser, D. Density functional theory with correct long-range asymptotic behavior. *Phys. Rev. Lett.* **2005**, *94*, 043002.

(21) Gerber, I. C.; Ángyán, J. G.; Marsman, M.; Kresse, G. Range separated hybrid density functional with long-range Hartree-Fock exchange applied to solids. *J. Chem. Phys.* **2007**, *127*, 054101.

(22) Livshits, E.; Baer, R. A well-tempered density functional theory of electrons in molecules. *Phys. Chem. Chem. Phys.* **2007**, *9*, 2932–2941.

(23) Baer, R.; Livshits, E.; Salzner, U. Tuned range-separated hybrids in density functional theory. *Annu. Rev. Phys. Chem.* **2010**, *61*, 85–109.

(24) Iikura, H.; Tsuneda, T.; Yanai, T.; Hirao, K. A long-range correction scheme for generalized-gradient-approximation exchange functionals. *J. Chem. Phys.* **2001**, *115*, 3540–3544.

(25) Vydrov, O. A.; Scuseria, G. E. Assessment of a long-range corrected hybrid functional. *J. Chem. Phys.* **2006**, *125*, 234109.

(26) Henderson, T. M.; Janesko, B. G.; Scuseria, G. E. Generalized gradient approximation model exchange holes for range-separated hybrids. *J. Chem. Phys.* **2008**, *128*, 194105.

(27) Weintraub, E.; Henderson, T. M.; Scuseria, G. E. Long-range-corrected hybrids based on a new model exchange hole. *J. Chem. Theory. Comput.* **2009**, *5*, 754–762.

(28) Chai, J.-D.; Head-Gordon, M. Systematic optimization of long-range corrected hybrid density functionals. *J. Chem. Phys.* **2008**, *128*, 084106.

(29) Heyd, J.; Scuseria, G. E.; Ernzerhof, M. Hybrid functionals based on a screened Coulomb potential. *J. Chem. Phys.* **2003**, *118*, 8207–8215.

(30) Chai, J.-D.; Head-Gordon, M. Long-range corrected hybrid density functionals with damped atom–atom dispersion corrections. *Phys. Chem. Chem. Phys.* **2008**, *10*, 6615–6620.

(31) Chai, J. D.; Head-Gordon, M. Long-range corrected double hybrid density functionals. *J. Chem. Phys.* **2009**, *131*, 174105.

(32) Mardirossian, N.; Head-Gordon, M. ωB97X-V: a 10-parameter, range-separated hybrid, generalized gradient approximation density functional with nonlocal correlation, designed by a survival-of-the-fittest strategy. *Phys. Chem. Chem. Phys.* **2014**, *16*, 9904–9924.

(33) Mardirossian, N.; Head-Gordon, M. ωB97M-V: A combinatorially optimized, range-separated hybrid, meta-GGA density functional with VV10 nonlocal correlation. *J. Chem. Phys.* **2016**, *144*, 214110.

(34) Mardirossian, N.; Head-Gordon, M. Survival of the most transferable at the top of Jacob's Ladder: defining and testing the ωB97M(2) double hybrid density functional. *J. Chem. Phys.* **2018**, *148*, 241736.

(35) Santra, G.; Cho, M.; Martin, J. M. L. Exploring avenues beyond revised DSD Functionals I: l. range separation, with xDSD as a special case. published as ArXiV preprint: arXiv:2102.04913 (accessed on 10 March 2021).

(36) Santra, G.; Semidalas, E.; Martin, J. M. L. Exploring avenues beyond revised DSD Functionals II: Random-Phase Approximation and scaled MP3 corrections. published as ArXiv preprint: arXiv:2102.04943 (accessed on 10 March 2021).

(37) Ángyán, J. G.; Gerber, I. C.; Savin, A.; Toulouse, J. Van der Waals forces in density functional theory: Perturbational long-range electron-interaction corrections. *Phys. Rev. A* **2005**, *72*, 012510.

(38) Benighaus, T.; DiStasio, R. A.; Lochan, R. C.; Chai, J.-D.; Head-Gordon, M. Semiempirical double-hybrid density functional with improved description of long-range correlation. *J. Phys. Chem. A* **2008**, *112*, 2702–2712.

(39) Zhang, I. Y.; Xu, X. Reaching a uniform accuracy for complex molecular systems:

long-range-corrected XYG3 doubly hybrid density functional. *J. Phys. Chem. Lett.* **2013**, *4*, 1669–1675.

(40) Kalai, C.; Toulouse, J. A general range-separated double-hybrid density-functional theory. *J. Chem. Phys.* **2018**, *148*, 164105.

(41) Mester, D.; Kállay, M. A Simple range-separated double-hybrid density functional theory for excited states. *J. Chem. Theory. Comput.* **2021**, *17*, 927–942.

(42) Casanova-Páez, M.; Dardis, M. B.; Goerigk, L. ωB2PLYP and ωB2GPPLYP: The first two double-hybrid density functionals with long-range correction optimized for excitation energies. *J. Chem. Theory. Comput.* **2019**, *15*, 4735–4744.

(43) Brémond, E.; Pérez-Jiménez, A. J.; Sancho-García, J. C.; Adamo, C. Range-separated hybrid density functionals made simple. *J. Chem. Phys.* **2019**, *150*, 201102.

(44) Brémond, E.; Savarese, M.; Pérez-Jiménez, A. J.; Sancho-García, J. C.; Adamo, C. Range-separated double-hybrid functional from nonempirical constraints. *J. Chem. Theory Comput.* **2018**, *14*, 4052–4062.

(45) Becke, A. D. Density-functional exchange-energy approximation with correct asymptotic behavior. *Phys. Rev. A* **1988**, *38*, 3098–3100.

(46) Lee, C.; Yang, W.; Parr, R. G. Development of the Colle-Salvetti correlation-energy formula into a functional of the electron density. *Phys. Rev. B* **1988**, *37*, 785–789.

(47) Casanova-Páez, M.; Goerigk, L. Assessing the Tamm–Dancoff approximation, singlet–singlet, and singlet–triplet excitations with the latest long-range corrected double-hybrid density functionals. *J. Chem. Phys.* **2020**, *153*, 064106.

(48) Goerigk, L.; Casanova-Paéz, M. The trip to the density functional theory zoo continues: making a case for time-dependent double hybrids for excited-State problems. *Aust. J. Chem.* **2021**, *74*, 3–15.

(49) Casanova-Páez, M.; Goerigk, L. Global double hybrids do not work for charge transfer: A comment on "Double hybrids and time-dependent density functional theory: An implementation and benchmark on charge transfer excited states". *J. Comput. Chem.* **2021**, *42*, 528–533.

(50) Karton, A.; Tarnopolsky, A.; Lamère, J.-F.; Schatz, G. C.; Martin, J. M. L. Highly accurate first-principles benchmark data sets for the parametrization and validation of density functional and other approximate methods. Derivation of a robust, generally applicable, double-hybrid functional for thermochemistry and thermochemical kinetics. *J. Phys. Chem. A* **2008**, *112*, 12868–12886.

(51) Perdew, J. P.; Burke, K.; Ernzerhof, M. Generalized gradient approximation made simple. *Phys. Rev. Lett.* **1996**, *77*, 3865–3868.

(52) Lonsdale, D. R.; Goerigk, L. The one-electron self-interaction error in 74 density functional approximations: a case study on hydrogenic mono- and dinuclear systems. *Phys. Chem. Chem. Phys.* **2020**, *22*, 15805–15830.

(53) Jana, S.; Śmiga, S.; Constantin, L. A.; Samal, P. Generalizing double-hybrid density functionals: impact of higher-order perturbation terms. *J. Chem. Theory Comput.* **2020**, *16*, 7413–7430.

(54) Grimme, S.; Antony, J.; Ehrlich, S.; Krieg, H. A consistent and accurate ab initio parametrization of density functional dispersion correction (DFT-D) for the 94 elements H-Pu. *J. Chem. Phys.* **2010**, *132*, 154104.

(55) Grimme, S.; Ehrlich, S.; Goerigk, L. Effect of the damping function in dispersion corrected density functional theory. *J. Comput. Chem.* **2011**, *32*, 1456–1465.

(56) Neese, F. The ORCA program system. *Wiley Interdiscip. Rev.: Comput. Mol. Sci.* **2012**, *2*, 73–78.

(57) Neese, F. Software update: the ORCA program system, version 4.0. *Wiley Interdiscip. Rev.: Comput. Mol. Sci.* **2017**, *8*, e1327.

(58) Weigend, F.; Ahlrichs, R. Balanced basis sets of split valence, triple zeta valence and quadruple zeta valence quality for H to Rn: Design and assessment of accuracy. *Phys. Chem. Chem. Phys.* **2005**, *7*, 3297–3305.

(59) Kendall, R. A.; Dunning, T. H.; Harrison, R. J. Electron affinities of the first-row atoms revisited. Systematic basis sets and wave functions. *J. Chem. Phys* **1992**, *96*, 6796–6806.

(60) Schwabe, T. Systematic study of the basis set superposition error in core–electron correlation effects. *J. Phys. Chem. A* **2013**, *117*, 2879–2883.

(61) Eichkorn, K.; Treutler, O.; Öhm, H.; Häser, M.; Ahlrichs, R. Auxiliary basis sets to approximate Coulomb potentials. *Chem. Phys. Lett.* **1995**, *240*, 283 – 290.

(62) DFT-D3 V3.1, S.Grimme, University of Bonn, 2014.

(63) Goerigk, L.; Grimme, S. Efficient and Accurate Double-Hybrid-Meta-GGA Density Functionals?Evaluation with the Extended GMTKN30 Database for General Main Group Thermochemistry, Kinetics, and Noncovalent Interactions. *J. Chem. Theory Comput.* **2011**, *7*, 291–309.

(64) Raghavachari, K.; Trucks, G. W.; Pople, J. A.; Head-Gordon, M. A fifth-order perturbation comparison of electron correlation theories. *Chem. Phys. Lett.* **1989**, *157*, 479–483.

(65) Taylor, D. E.; Ángyán, J. G.; Galli, G.; Zhang, C.; Gygi, F.; Hirao, K.; Song, J. W.; Rahul, K.; Anatole von Lilienfeld, O.; Podeszwa, R. et al. Blind test of density-functional-based methods on intermolecular interaction energies. *J. Chem. Phys.* **2016**, *145*, 124105.

(66) Gráfová, L.; Pitoňák, M.; Řezáč, J.; Hobza, P. Comparative study of selected wave function and density functional methods for noncovalent interaction energy calculations using the extended S22 data set. *J. Chem. Theory Comput.* **2010**, *6*, 2365–2376.

(67) Řezáč, J.; Riley, K. E.; Hobza, P. S66: A well-balanced database of benchmark interaction energies relevant to biomolecular structures. *J. Chem. Theory Comput.* **2011**, *7*, 2427–2438.

(68) Caldeweyher, E.; Bannwarth, C.; Grimme, S. Extention of the D3 dispersion coefficient model. *J. Chem. Phys.* **2017**, *147*, 034112.

(69) Caldeweyher, E.; Ehlert1, S.; Hansen, A.; Neugebauer, H.; Spicher, S.; Bannwarth, C.; Grimme, S. A generally applicable atomic-charge dependent London dispersion correction. *J. Chem. Phys.* **2019**, *150*, 154112.

(70) Grimme, S.; Hansen, A.; Brandenburg, J. G.; Bannwarth, C. Dispersion-corrected mean-field electronic structure methods. *Chem. Rev.* **2016**, *116*, 5105–5154.

(71) Goerigk, L. In *Non-Covalent Interactions in Quantum Chemistry and Physics*; Otero de la Roza, A., DiLabio, G. A., Eds.; Elsevier: Amsterdam, 2017; pp 195 – 219.

(72) Kozuch, S.; Martin, J. M. L. Spin-component-scaled double hybrids: An extensive search for the best fifth-rung functionals blending DFT and perturbation theory. *J. Comput. Chem. 34*, 2327–2344.

(73) Schwabe, T.; Goerigk, L. Time-dependent double-hybrid density functionals with spin-component and spin-opposite scaling. *J. Chem. Theory Comput.* **2017**, *13*, 4307–4323.

(74) Curtiss, L. A.; Raghavachari, K.; Trucks, G. W.; Pople, J. A. Gaussian-2 theory for molecular energies of first- and second-row compounds. *J. Chem. Phys.* **1991**, *94*, 7221–7230.

(75) Goerigk, L.; Grimme, S. A general database for main group thermochemistry, kinetics and noncovalent interactions — assessment of common and reparameterized (meta-)GGA density functionals. *J. Chem. Theory Comput.* **2010**, *6*, 107–126.

(76) Vydrov, O. A.; Heyd, J.; Krukau, A. V.; Scuseria, G. E. Importance of short-range versus long-range Hartree-Fock exchange for the performance of hybrid density functionals. *J. Chem. Phys.* **2006**, *125*, 074106.

(77) Chai, J.-D.; Mao, S.-P. Seeking for reliable double-hybrid density functionals without fitting parameters: The PBE0-2 functional. *Chem. Phys. Lett.* **2012**, *538*, 121 – 125.

(78) Song, S.; Vuckovic, S.; Sim, E.; Burke, K. Density sensitivity of empirical functionals. *J. Phys. Chem. Lett.* **2021**, *12*, 800–807.

(79) Santra, G.; Martin, J. M. L. What types of chemical problems benefit from density-corrected DFT? A probe using an extensive and chemically diverse test suite. *J. Chem. Theory. Comput.* **2021**, published online, DOI: 10.1021/acs.jctc.0c01055 (accessed on 16 March 2021).

Graphical TOC Entry